Journal of Power Sources 196 (2011) 4080–4087

Contents lists available at ScienceDirect

Journal of Power Sources

journal homepage: www.elsevier.com/locate/jpowsour

Concentrated $NaClO_4$ aqueous solutions as promising electrolytes for electric double-layer capacitors

Jiao Yin [a,b], Cheng Zheng [a,b], Li Qi [a], Hongyu Wang [a,*]

[a] State Key Laboratory of Electroanalytical Chemistry, Changchun Institute of Applied Chemistry, Chinese Academy of Sciences, 5625 Renmin Street, Changchun 130022, China
[b] Graduate University of Chinese Academy of Sciences, Beijing 100039, China

ARTICLE INFO

Article history:
Received 19 October 2010
Received in revised form 6 December 2010
Accepted 16 December 2010
Available online 24 December 2010

Keywords:
Porous carbon electrodes
Electric double-layer capacitors
$NaClO_4$ aqueous solutions
Electrolytes
Raman spectra

ABSTRACT

Concentrated $NaClO_4$ aqueous solutions have been proposed as the electrolytes in electric double-layer capacitors. The advantages of this kind of electrolytes have been addressed in the terms of enlarged specific capacitance, enhanced rate capability and elevated low-temperature performance of porous carbon electrodes. Thermal analysis, ionic conductivity measurement and Raman spectroscopic investigations have been performed on the $NaClO_4$ aqueous solutions in conjunction with the electrochemical study of porous carbon electrodes in this kind of electrolytes. The correlation between the hydration number of ions in the solutions and capacitive behavior of porous carbon has been clarified. The rate performance improvement in porous carbon electrode has also been connected to the increase in ionic conductivity of the electrolytes. The enhanced capacitance retention of porous carbon electrode at low temperatures in concentrated solutions has been ascribed to a fall of freezing point.

1. Introduction

During the past decades, the progressive advocacy of electric double-layer capacitors (EDLCs) as a major member in the community of electric storage devices has been witnessed. As a contemporary, EDLCs are always overshadowed by lithium-ion batteries in the terms of energy density. To cover the Achilles heel of EDLCs, numerous studies have been carried out on how to increase their energy density. Most efforts have been devoted to electrode materials with porous or nano-sized structures. From the viewpoint of electrolyte, the electrochemical window is always considered as a predominant factor since the energy density of an electrochemical capacitor is proportional to the square of its working voltage, thus non-aqueous electrolytes possessing broader electrochemical windows appear more suitable in "high-energy" capacitors [1].

For many practical applications, the needs to elevate energy density of EDLCs may be overstated somehow. Alternatively, more attention should be redrawn to how can make good use of its virtue, the high power density. In this sense, aqueous electrolyte solutions become more competitive in the practical applications of electrochemical capacitors because of the following merits: low cost, easy manipulation, green chemistry, safety, high conductivity (high power density), etc. In addition, the energy density of electrochemical capacitor can be compensated somewhat by the usage of aqueous electrolytes in spite of its narrow working voltage range within 1.2 V since a porous carbon electrode generally delivers higher specific capacitance values in aqueous electrolytes than in non-aqueous electrolytes. (The energy density of an electrochemical capacitor is also proportional to its capacitance).

Then the main problem with aqueous electrolytes probably lies in the "high" freezing point of water solvent, which may limit the utilization of electrochemical capacitors at low temperatures. Concentrated electrolyte solutions can overcome this obstacle apparently. In the previous studies on electrochemical capacitors, the aqueous solutions containing concentrated acidic or alkaline electrolytes (like 10 M H_2SO_4 or 6 M KOH) have always been employed. However, they are too caustic to handle. Therefore, milder neutral aqueous solutions based on safe and highly soluble alkali salts may be satisfactory candidates for electrolytes. Table 1 lists a variety of neutral salts as aqueous electrolytes for electrochemical capacitors in the published literatures. $LiNO_3$ can be highlighted because of the solubility as high as 9 M [1]. To our surprise, there are rare reports relates to another highly soluble neutral salt, $NaClO_4$ (up to 5 M soluble in aqueous solutions) as the electrolyte in electrochemical capacitors. In the terms of anodic stability, $NaClO_4$ is superior to $LiNO_3$, which advantage may guarantee the long cycle life and safety of electrochemical capacitors if they are overcharged by accident. On the other hand, the performance of electrochemical capacitors using highly concentrated electrolyte solutions needs further investigations. In their systematic studies on the limitation of energy density by the salt concentration,

* Corresponding author. Tel.: +86 431 85262287; fax: +86 431 85262287.
E-mail addresses: wanghongyu@hotmail.com, hongyuwang@ciac.jl.cn (H. Wang).

0378-7753/$ – see front matter © 2010 Elsevier B.V. All rights reserved.
doi:10.1016/j.jpowsour.2010.12.064

Table 1
Summary of the various classes of aqueous neutral salts investigated.

Neutral salts	C, mol L^{-1}	Operating voltage, V	Electrode materials	Current density or scan rate	Specific capacitance or capacity	References
$LiNO_3$	0.1	1	AC	0.2 mV s^{-1}	24 μF cm^{-1}	[2a]
	Saturated	1.05	$LiV_3O_8/LiCoO_2$	0.2 mA cm^{-2}	55 mAh g^{-1}	[3]
	1	1.1	$LiMn_2O_4$	500 mA cm^{-1}	108.3 mAh g^{-1}	[2b]
	5	1.1	$LiMn_2O_4$	500 mA cm^{-1}	119.1 mAh g^{-1}	[2b]
	9	1.1	$LiMn_2O_4$	500 mA cm^{-1}	121.6 mAh g^{-1}	[2b]
	5	1	$LiMn_2O_4$	109 mA cm^{-1}	73 mAh g^{-1}	[4]
	2	1	AC/V_2O_5	200 mA cm^{-1}	29.9 Fg^{-1}	[5]
$NaNO_3$	2	1	AC/V_2O_5	200 mA cm^{-1}	32.5 Fa^{-1}	[5]
KNO_3	2	1	AC/V_2O_5	200 mA cm^{-1}	31.5 Fg^{-1}	[5]
	2	1.2	AC	2 mV s^{-1}	200 Fg^{-1}	[6]
	2	0.6	a-MnO_2-CNT	250 mA cm^{-1}	140 Fg^{-1}	[7]
LiCl	1	0.6	AC	40 m Ag^{-1}	145 Fg^{-1}	[8]
	2	1.2	MnO_2	5 mV s^{-1}	59 Fg^{-1}	[9]
	2	1	MnO_2	2 mV s^{-1}	180 Fg^{-1}	[10]
NaCl	0.2	1.2	AC	2 mV s^{-1}	20 μF cm^{-2}	[2]
	2	1.2	MnO_2	5 mV s	138 Fg^{-1}	[9]
	2	1	MnO_2	2 mV s^{-1}	248 Fg^{-1}	[10]
KCl	2	1.2	MnO_2	5 mV s^{-1}	109 Fg^{-1}	[9]
	2	1	MnO_2	2 mV s^{-1}	195 Fg^{-1}	[10]
	1	1.6	AC	10 mV s^{-1}	210 Fg^{-1}	[11]
	1	1	MnO_2-CNT	10 Ag^{-1}	500 Fg^{-1}	[12]
	1	0.8	AC/MnO_2	2 mV s^{-1}	144 Fg^{-1}	[13]
$LiClO_4$	0.1	0.9	AC	0.2 mV s^{-1}	15 μF cm^{-1}	[2]
$NaClO_4$	5	1.2	AC	5 mV s^{-1}	158 Fg^{-1}	Our result in this study
Li_2SO_4	*2*	1.1	$LiMn_2O_4$	500 mA Ag^{-1}	114 Fg^{-1}	[2a]
	1	1	AC/V_2O_5	200 mA Ag^{-1}	25.1 Fg^{-1}	[5]
	0.5	1.3	AC	1 mV s^{-1}	115 Fg^{-1}	[14]
	1	1.8	$AC/LiMn_2O_4$	3 mA cm^{-2}	40–80 mAh g^{-1}	[15]
	0.5	1	MnO_2	1 mV s^{-1}	201 Fg^{-1}	[16]
	1	2.5	AC/MnO_2	100 m Ag^{-1}	60 Fg^{-1}	[17]
Na_2SO_4	1	1	AC/V_2O_5	200 m Ag^{-1}	29.3 Fg^{-1}	[5]
	0.1	1	MnO_2	2 mV s^{-1}	188 Fg^{-1}	[10]
	0.5	1.3	AC	1 mV s^{-1}	113 Fg^{-1}	[14]
	0.5	1	MnO_2	1 mV s^{-1}	185 Fg^{-1}	[16]
	1	2.8	AC	20 mV s^{-1}	75 Fg^{-1}	[18]
	0.1	1	SnO_2	10 mV s^{-1}	285 Fg^{-1}	[19]
	1	1	Ni–Mn oxide	10 mV s^{-1}	621 Fg^{-1}	[20]
	1	1	Co–Mn oxide	10 mV s^{-1}	498 Fg^{-1}	[20]
	0.1	1	Polyaniline–MnO_2	5 mA cm^{-2}	715 Fg^{-1}	[21]
	0.1	0.9	MnO_2	2 mV s^{-1}	180 Fg^{-1}	[22]
	1	0.8	MnO_2	2 mV s^{-1}	188 Fg^{-1}	[23]
	0.1	1	$MtiO_2$	10 mV s^{-1}	482 Fg^{-1}	[24]
	1	1	AC/V_2O_5	200 mA Ag^{-1}	28 Fg^{-1}	[5]
K_2SO_4	0.5	1.3	AC	1 mV s^{-1}	110 Fg^{-1}	[14]
	0.5	1	MnO_2	1 mV s^{-1}	175 Fg^{-1}	[16]
	0.5	0.8	MnO_2	0.5 mAcm^{-2}	229 Fg^{-1}	[25]
	0.65	1.3	MnO_2	5 mV s^{-1}	150 Fg^{-1}	[26]
	0.65	1.3	AC	5 mV s^{-1}	120 Fg^{-1}	[26]
	0.1	0.9	MnO_2	2 mV s^{-1}	72 Fg^{-1}	[27]
	0.1	1.1	AC	2 mV s^{-1}	95 Fg^{-1}	[27]
	0.1	1	MnO_2	5 mV s^{-1}	150 Fg^{-1}	[28]
	0.1	0.9	Fe_3O_4	5 mV s^{-1}	75 Fg^{-1}	[28]

Zheng et al. [29–31] proposed that charging electrochemical capacitors will significantly deplete the "free" ions in the bulk solution of electrolyte and accumulate a big amount of ions near the electrolyte/electrode interfaces. To make sure of the smooth operation of electrochemical capacitors, sufficient electrolytes should be contained to satisfy the charge storage ability of electrodes. This is the reason why electrolyte solutions with high concentrations are generally used in practical electrochemical capacitors. However, in most cases, the neutral salt concentrations in aqueous solutions were not very high (<2 M), only if the total amount of ions in the electrolyte solutions is large enough for the full adsorption capability of electrodes. Moreover, the properties of electrolyte aqueous solutions in electrochemical capacitors are roughly evaluated by the classic theories of the dilute electrolyte solutions [32]. In fact, the hydration states of ions at high concentrations of electrolytes are quite different from those in dilute solutions. Each ion will be hydrated by limited numbers of water molecules, which case is somewhat similar to ionic liquid. Then the volume of each charge carrier (hydrated ions) will shrink as the hydration number becomes smaller, which fact may contribute to the increase in the adsorption capability (capacitance) of electrodes. From the view point of Debye length, Huang et al. [33] have roughly estimated the same trend.

Bearing the above estimations in mind, we attempted to explore a "versatile" electrolyte for electrochemical capacitors based on concentrated $NaClO_4$ aqueous solutions in this study. The effect of $NaClO_4$ concentration on the electrochemical performance of porous carbon electrodes and the total electric double-layer capacitors has also been addressed.

2. Experimental

2.1. Characterization of electrolyte solutions

Raman spectra of various $NaClO_4$ aqueous solutions were measured with a Renishaw 2000 model confocal microscopy Raman

spectrometer with a CCD detector and a holographic notch filter. Radiation of 514.5 nm from an air-cooled argon ion laser was used for the Raman excitation. The conductivities of the $NaClO_4$ aqueous solution were measured by Conductivity meter DDS-11A. The viscosity at 25 °C was measured using an Ostwald viscometer. Differential scanning calorimetry (DSC) was used to measure freezing points by PerkinElmer Thermal analysis instrument.

2.2. Preparation of electrodes

The porous carbon electrode material used in this paper was Maxsorb, with the B.E.T. specific surface area of 1333 $m^2 g^{-1}$. From its pore size distribution as shown in Fig. 2, the micro-porous feature ranges from 0.5 to 2 nm can be clearly observed. Maxsorb electrodes were fabricated by pressing the mixture of Maxsorb and TAB (teflonized acetylene black) on each stainless steel mesh (1 cm^2 area).

2.3. Electrochemical measurements

Cyclic voltammetric studies were carried out on three-electrode beaker cells by CHI700D potentiostat/galvanostat. A three-electrode cell comprises a Maxsorb working electrode, a platinum flag counter electrode, and a Ag/AgCl (saturated KCl) reference electrode. Galvanostatic charge–discharge cycles of two-electrode beaker cells were measured by a Land cell tester. The cutoff voltages were set at 0 and 1.2 V. In a two-electrode cell, both the positive and negative electrodes were Maxsorb electrodes. $NaClO_4$ aqueous solutions with different concentrations were used as the electrolytes.

3. Results and discussion

Raman spectroscopy is a powerful technique to investigate the structures and interactions of ions in solvents. Fig. 1A com-

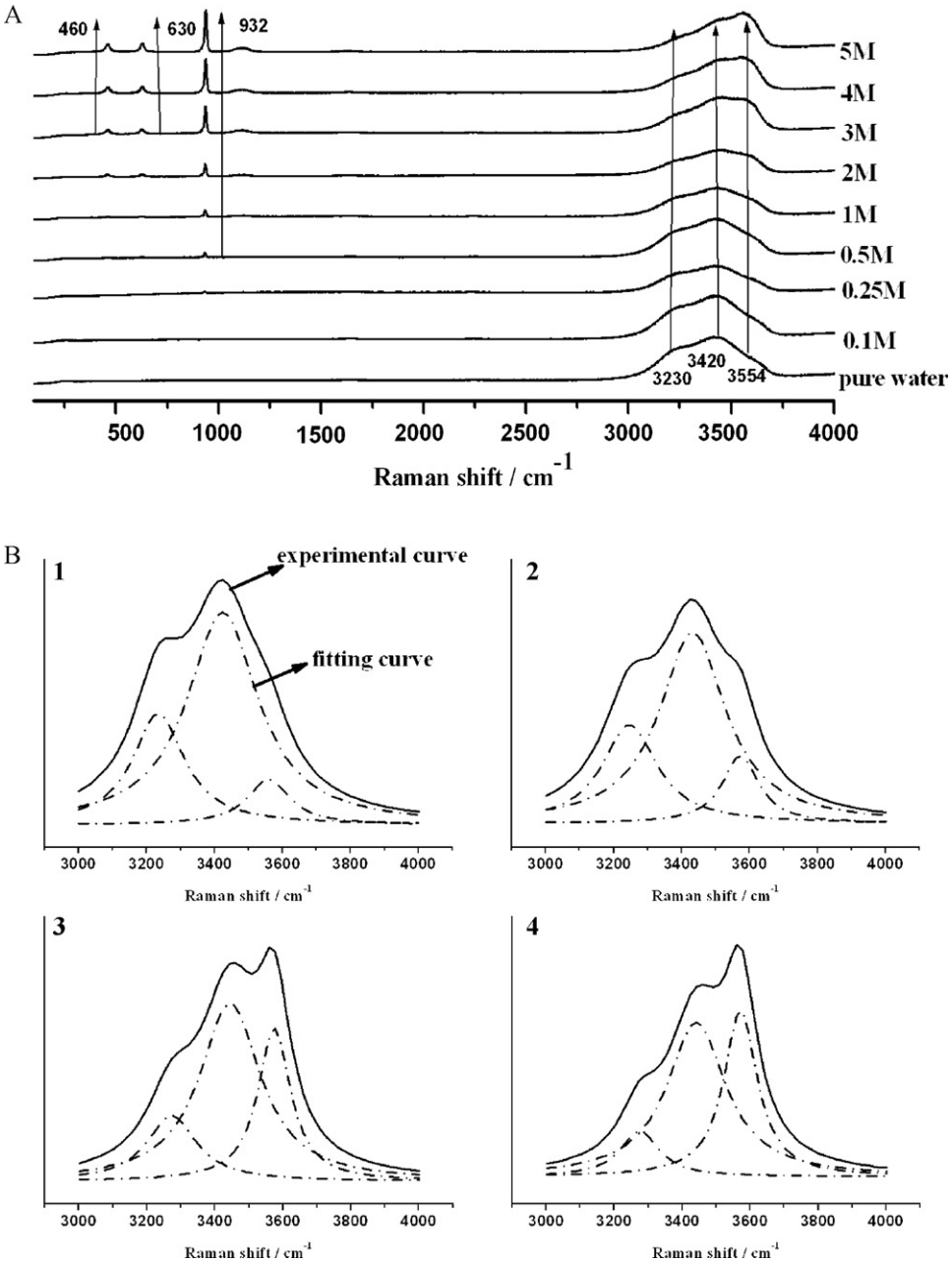

Fig. 1. (A) Raman spectra of pure water and 0.1–5 M $NaClO_4$ aqueous solutions, (B) Lorentzian peak fitting from the frequency of 3000–4000 cm^{-1}: (1) pure water, (2) 1 M, (3) 3 M, (4) 5 M $NaClO_4$ aqueous solutions, respectively.

Table 2
Raman band shift of ν_1 (932 cm^{-1}).

C, mol L^{-1}	0.1	0.25	0.5	1	2	3	4	5
Band shift, cm^{-1}	932.3	933.1	933.7	935.1	935.1	935.1	936.5	936.5

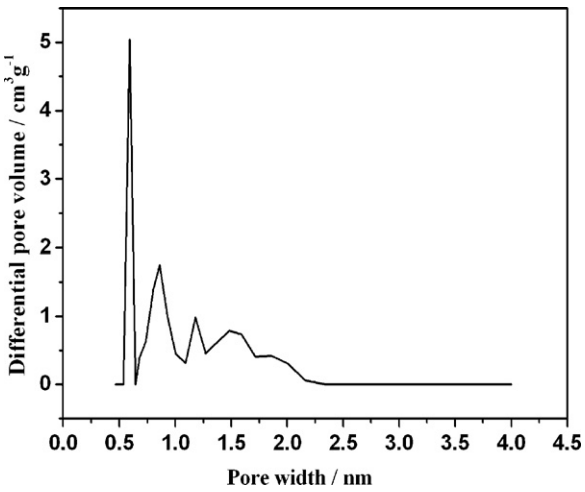

Fig. 2. Pore size distribution of Maxsorb.

pares the Raman spectra of $NaClO_4$ aqueous solutions. In the spectra of 400–1200 cm^{-1}, the four bands are signatures corresponding to the vibration modes of ClO_4^-. The free perchlorate anions are of tetrahedral (T_d) symmetry and show four fundamental vibration bands: symmetric stretching band at ~932 cm^{-1} (ν_1, A_1, nondegenerate, R), symmetric bending band at ~460 cm^{-1} (ν_2, E, doubly degenerate, R), asymmetric stretching band at ~1115 cm^{-1} (ν_3, F_2, triply degenerate, IR and R), asymmetric bending band at ~630 cm^{-1} (ν_4, F_2, triply degenerate, IR and R) where IR and R denote infrared and Raman activity respectively [35,36]. As is shown in Fig. 2, ν_1, ν_2, ν_4, bands remain available. Therefore, we focused on the 400–1000 cm^{-1} region to observe the state of ClO_4^-. Ion–solvent interaction in the Raman spectra of perchlorate solutions have been identified [35–40]. Four species have been identified: (1) free ClO_4^- anions (at 930 cm^{-1}); (2) solvent separated ion pairs M^+–solvent–ClO_4^- (at 939 cm^{-1}); (3) contact ion pairs M^+ ClO_4^-, (at 948 cm^{-1}); (4) multiple ion aggregates $\{M^+ ClO_4^-\}_n$ (at 955 cm^{-1}). In the present investigation, the band (ν_1) shifts from 932 to 937 cm^{-1} shown in Table 2 at the concentration interval of 0.1–5 M. This is attributed to gradually forming the solvent separated ion pair $\{Na^+ (H_2O)_n ClO_4^-\}$, and its intensity increases with increasing $NaClO_4$ content. These species are larger in size and hence reduce the mobility of ions and increase the viscosity of solutions, hence, the conductivity is not dramatically increased above 3 M, which will be discussed in the following parts. Furthermore, ClO_4^- has "structure breaking" effect on the hydrogen bond network of water as reflected in ATR-FTIR and Raman Spectroscopy [35,36]. Consequently, the O–H stretching envelope of water in $NaClO_4$ aqueous solution is affected by Na^+ and ClO_4^-. In pure liquid water, the O–H stretching envelope is generally composed of four components, attributed to an ice-like component (C_1) at ~3230 cm^{-1}, an ice-like liquid component (C_2) at ~3420 cm^{-1}, a liquid like amorphous phase (C_3) at ~3540 cm^{-1}, and monomeric H_2O (C_4) at ~3620 cm^{-1}, of which the two on the low wavenumber sides are assigned to the water molecules with fully hydrogen-bonded five-molecule tetrahedral nearest neighbor structure and the one on the high wavenumber side to the water monomers with no or weak hydrogen bonds. In our investigations, the Raman shift of water mainly concentrate on 3000–3600 cm^{-1} and the peak at ~3620 cm^{-1} can both be observed in Raman shift. The O–H stretching bands of 3230 cm^{-1} and 3420 cm^{-1} can be used as characters for pure liquid water. The two bands can be clearly observed in the spectra of pure water. With increasing $NaClO_4$ salt concentration, these Raman spectra change their shapes and intensities. From 0 to 1 M, the shapes of Raman spectra show no obvious differences, the O–H stretching bands of 3230 cm^{-1} and 3420 cm^{-1} are still pronounced and their intensities gradually decrease and can be obtained by the Lorentzian curve fitting shown in Fig. 1B. When the concentrations increase to 3 M, the peaks start to split, the band of 3554 cm^{-1} can be observed. From 3 to 5 M, this band is visuable and becomes main peak shown in Fig. 1B, which is mainly owing to "structure breaking" effect of ClO_4^- on the hydrogen bond network of water and the intensity decrease of 3230 cm^{-1} and 3420 cm^{-1}. This trend indicates that hydrogen bonds of water are obviously broke with the increase of $NaClO_4$. The changes of the low wavenumber sides (3100–3300 cm^{-1}) mainly are the results of cationic effects on the Raman O–H stretching spectrum of water according to the reported literatures [35,41]. The one on the high wavenumber side 3540 cm^{-1} is also affected by ClO_4^-. As a result, we can estimate the number of water molecules strongly bound to a Na^+ cation (hydration number) from the results of Raman spectral measurements and analyses by the band decrease of ~3230 cm^{-1}. The hydration number (N_h) can be deduced from the following Eq. (1) and (2) [36,41,42]:

$$M_h = \left(\frac{\Delta I}{I_{3230}}\right) C_w \quad (1)$$

$$N_h = \frac{M_h}{C_h} \quad (2)$$

where are the intensities of pure water and different concentrations of $NaClO_4$ on the wavenumber side of 3230 cm^{-1}. C_w and C_h are the concentrations of H_2O and $NaClO_4$, respectively, and M_h is the concentration of H_2O molecules strongly bound to Na^+. The results are given in Table 3.

Table 3
Estimation of hydration numbers.

C_{NaCio4}, mol L^{-1}	Apparent Na^+:H_2O molar ratio	Raman fitting intensity ratio $\Delta I/I_{3230}$	Hydration numbers of Na^+ from Raman spectra (N_h)	Apparent n_{H2O}/n_{NaCiO4} from theoretical calculation
0.1	0.0018	0.15	81	543
0.25	0.0047	0.31	67	215
0.5	0.0096	0.34	35	104
1	0.0196	0.35	18	51
2	0.0417	0.36	9	24
3	0.0667	0.38	6	15
4	0.0909	0.49	5	11
5	0.1429	0.61	4	7

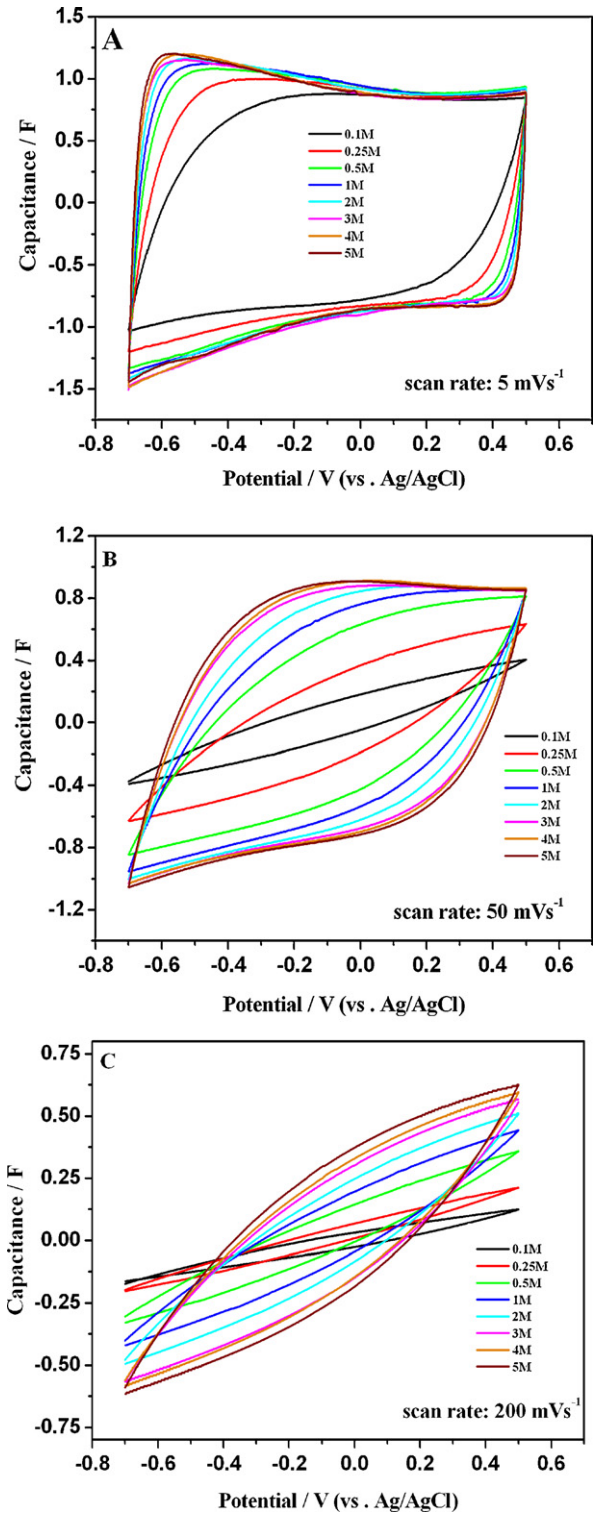

Fig. 3. Cyclic voltammograms of Maxsorb electrode in $NaClO_4$ aqueous solutions with different concentrations at room temperature (25 °C) at the scan rates of 5 mV s^{-1} (A), 50 mV s^{-1} (B), and 200 mV s^{-1} (C), respectively.

Fig. 2 shows the pore size distribution of the Maxsorb. It is typically microporous with a pore size distribution range from 0.5 to 2 nm. Some physical properties of this porous carbon has been described in our previous study [34].

Cyclic voltammetry (CV) has been frequently applied to evaluate the capacitive behavior of electrode materials in electrochemical capacitors. Fig. 3 compares the cyclic voltammograms of Maxsorb electrode in $NaClO_4$ aqueous solutions with different concentrations at room temperature (25 °C) at the scan rates of 5, 50, and 200 mV s^{-1}, respectively. At each scan rate, the area surrounded by the CV curve becomes larger with the rise in $NaClO_4$ concentration. This implies the following trend: the higher the concentration of $NaClO_4$, the bigger the specific capacitance (SC) values of Maxsorb electrode. Here the total amount of ions in each 20 mL solution

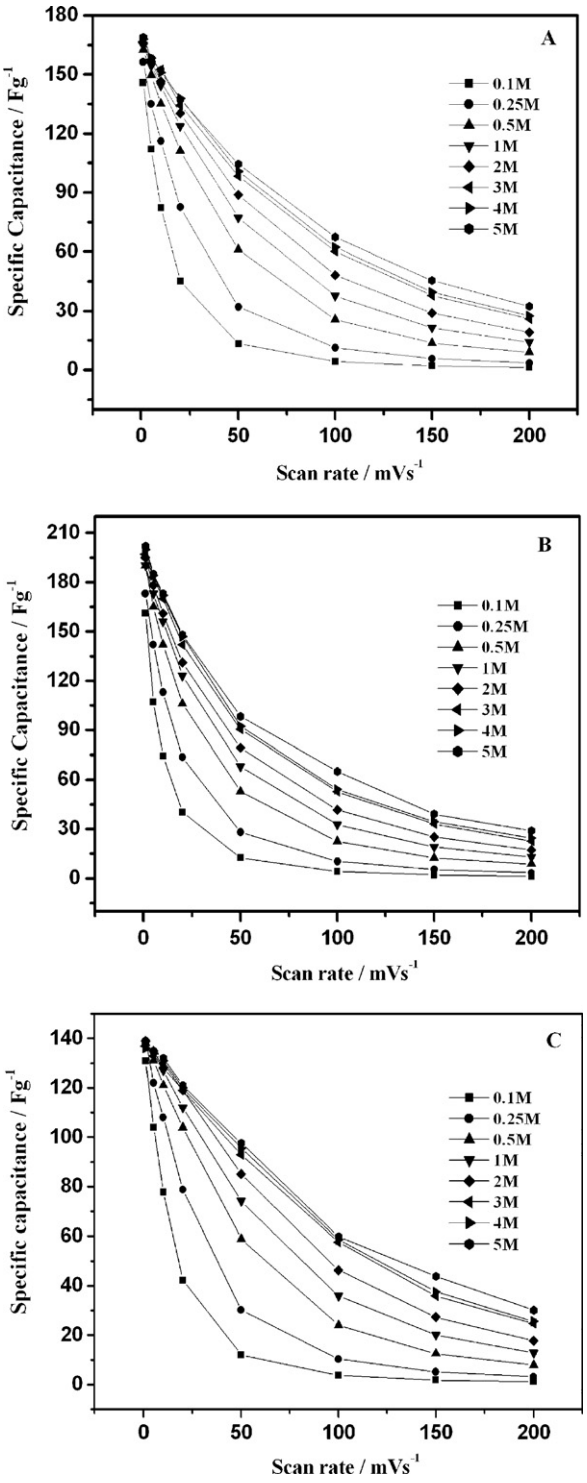

Fig. 4. Relationships between the specific capacitance values and scan rate at different salt concentrations. Note: The inset symbols "total (A)", "− (B)", and "+ (C)" stand for the potential ranges from −0.7 to 0.5 V, −0.7 to −0.2 V and 0 to 0.5 V vs. Ag/AgCl, respectively.

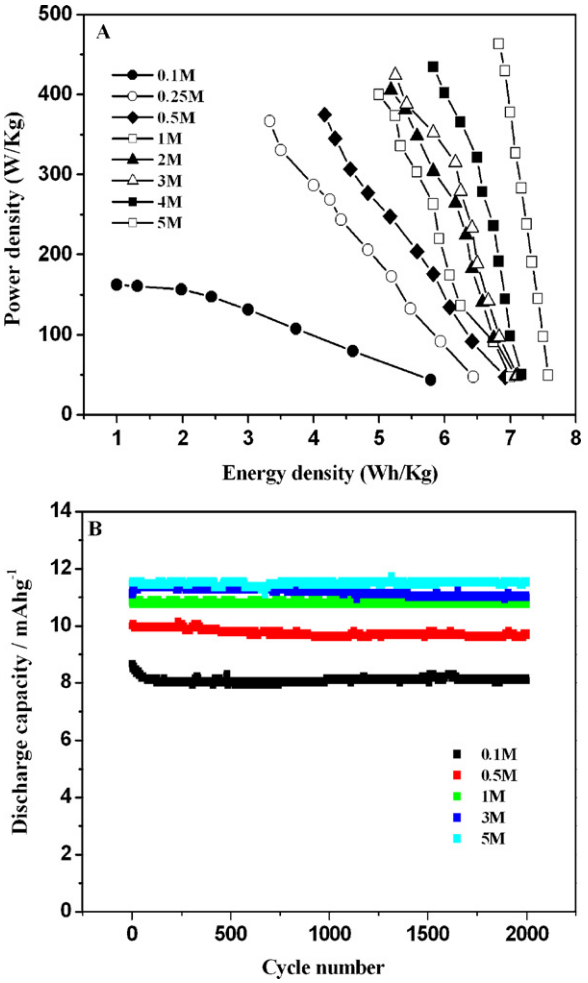

Fig. 5. (A) Ragone plot of two symmetrical Maxsorb electrodes with different concentrations of $NaClO_4$ and (B) Cycle performance of different capacitors at the constant current density of 166.67 mA/g. The discharge capacity values were calculated by taking account the total mass of both electrode active materials in each capacitor.

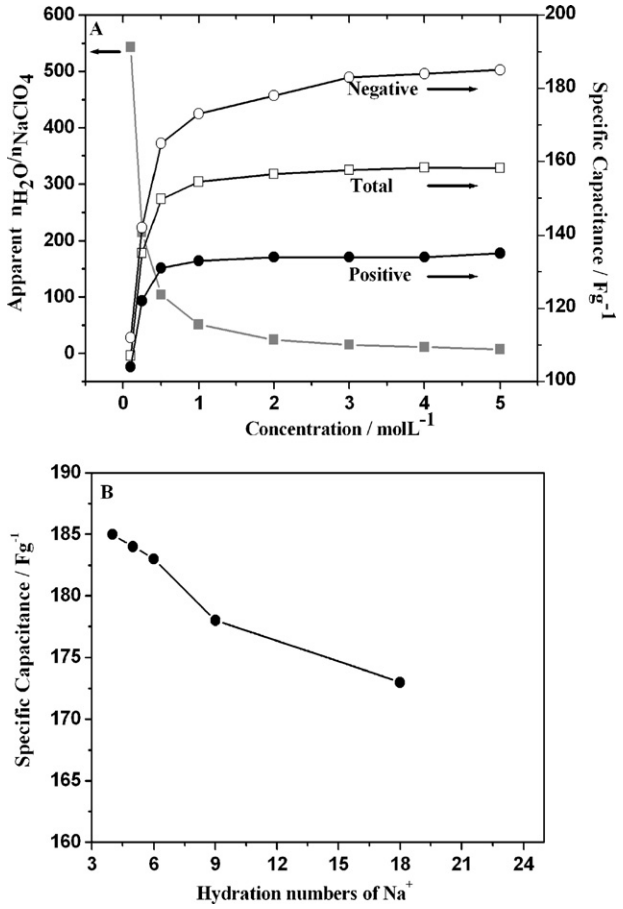

Fig. 6. Relationship between ionic conductivity (A) and viscosity (B), and salt concentration. The conductivity and viscosity were measured at 25 °C.

actually overwhelms the maximum charge storage ability of a Maxsorb electrode (6 mg Maxsorb) even at the minimum concentration of salt (0.1 M). Therefore, the possibility of ions shortage in the bulk electrolyte solution as proposed by Zheng et al. [29] can be excluded. From the cyclic voltammograms, the SC values of Maxsorb electrode can be calculated as described in the previous study [34]. Fig. 4 depicts the relationships between the SC values and scan rates at different salt concentrations. In all the potential ranges, a common feature can be observed. The curve representing higher salt concentration usually locates at a higher position of SC values. This implies that in the concentrated $NaClO_4$ aqueous solutions, not only the SC value but also the rate performance have been elevated. The former parameter is a key indicator of energy density, whereas the latter trait is characteristic of power density for the electrochemical capacitors. Fig. 5A shows the Ragone plot of electric double-layer capacitors composed of two symmetrical Maxsorb electrodes and $NaClO_4$ aqueous solutions. The calculation methods of energy and power densities, discharge capacity by galvanostatic charge-discharge curves have been reported in the literature [34]. The electric double-layer capacitors using concentrated electrolytes have both higher energy and power densities. Furthermore, the long cycle performances of the above capacitors are shown in Fig. 5B, it reveals that concentrated salts deliver much bigger energy density and all these five capacitors have stable cycle life.

The improvement in power density accompanying the rise in salt concentration can be mainly ascribed to the increase in ionic conductivity. Fig. 6A shows the relationship between ionic conductivity and salt concentration. The curve demonstrates an arc shape with the maximum conductivity at the concentration between 4 and 5 M. Of course, the monotonic increase in charge carriers (ions) number in the electrolyte solution contributes to the conductivity enhancement to a big extent. However, the appearance of the maximum value implies that another factor also affects the conductivity negatively. In the Raman spectra of $NaClO_4$ solutions, we noticed that the shift of ClO_4^- (ν_1) vibration band from 932 to 937 cm^{-1} as the salt concentration rises from 0.1 to 5 M. This fact implies the formation of complex ion aggregations, and the electrolyte solutions get more viscous. The rise in the viscosity (η) actually retards the mobility of ions. So we also plotted the relationship between the quotient of salt concentration/viscosity and concentration in Fig. 6B. This curve has very similar tendency to that corresponding to ionic conductivity vs. salt concentration. The improvement in energy density with the rise in salt concentration is actually due to the enhancement of SC values. Fig. 7A shows the relationship between SC values and the salt concentration. Here the SC values were obtained from the cyclic voltammetric results at 5 mV s^{-1} since the kinetic influence becomes negligible at the slow scan rate. Moreover, these values were measured in three potential ranges: the positive potential range corresponding to the adsorption of anions, the negative potential range corresponding to the adsorption of cations, and the total potential range. In all the potential ranges, the SC values rise drastically as the salt concentration shifts from 0.1 to 0.5 M. As the salt concentration exceeds 1 M, the climb-up tendency of

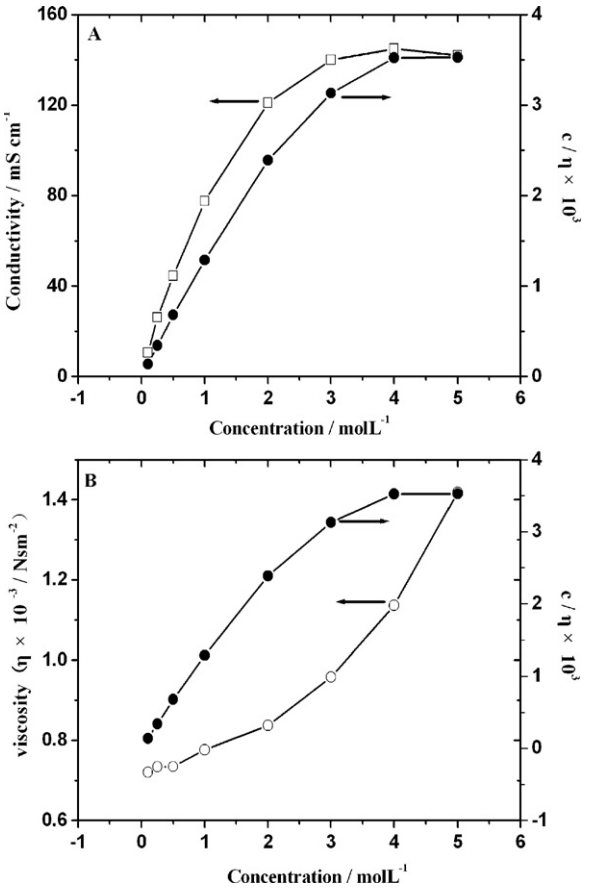

Fig. 7. (A) Relationship between SC values, n_{H2O}/n_{NaClO4}, and the salt concentration. Note: The inset symbols "negative", "total" and "positive" stand for the potential ranges from −0.7 to −0.2 V, −0.7 to 0.5 V and 0 to 0.5 V vs. Ag/AgCl, respectively, (B) Relationship between the SC values in the negative potential range and the hydration number of Na^+ in the concentrated electrolyte solutions (1–5 M).

SC values is slowed down. The SC value in the positive potential range almost levels off at higher salt concentrations. By contrast, the SC value in the negative potential range increases by about 8% from 1 to 5 M. The molecular number ratio of solvent to salt (n_{H2O}/n_{NaClO4}) is strongly dependent on the salt concentration. This curve drops down sharply at first in the low salt concentration region, and then decays sluggishly in the high salt concentration region. It looks like a mirror image of the curves corresponding to the SC values shown in Fig. 7A. From the classic Stern model of double layer, the direct response of SC values to the salt concentration in dilute electrolyte solutions may be roughly explained by the diffuse-charge capacitance in Gouy-Chapman region. On the other hand, in concentrated electrolyte solutions (1–5 M), the SC values may be primarily controlled by the capacitance in Helmholtz region, which closely relates to the hydration number of ions that are adsorbed in the pores of Maxsorb electrodes. The plateau portion (1–5 M) in the curve corresponding to the positive potential range means that there is little change in the adsorption capability of hydrated ClO_4^- anions on Maxsorb electrode. By contrast, in the same concentration region, the SC value for the negative potential range is not constant, but becomes considerably larger as the salt concentration increases. Raman spectral results in Table 3 have shown that the hydration number of Na^+ in the bulk electrolyte solution gets smaller as the salt concentration rises. It is expected that the shrinkage in the guest (hydrated Na^+) size will increase the accommodation amounts of guest in the same host (the pores of Maxsorb). Fig. 7B plots the relationship between the SC values in the negative potential range and the hydration number of Na^+

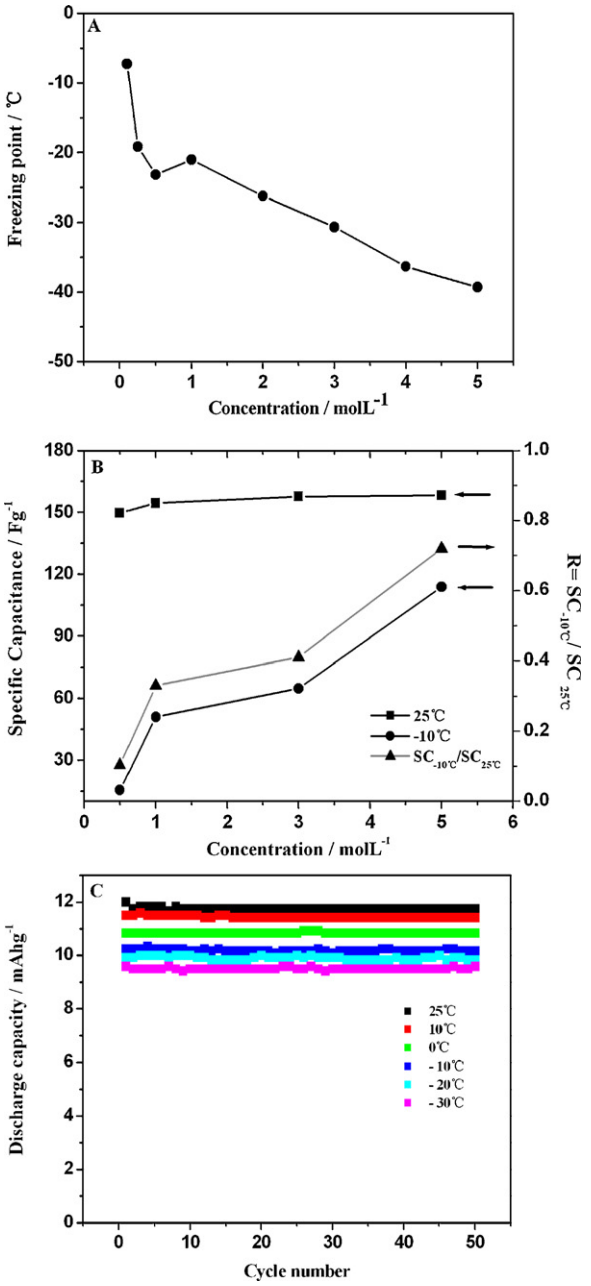

Fig. 8. (A) Relationship between the freezing point and the salt concentration of the electrolyte solution, (B) SC values of a Maxsorb electrode at the temperatures of 25 and −10 °C in the aqueous electrolyte solutions with various $NaClO_4$ concentrations and (C) the discharge capacity of capacitor in the electrolyte of 5 M $NaClO_4$ aqueous solution at different temperatures (the charge and discharge current density at 166.67 mA/g). The discharge capacity values were calculated by taking account the total mass of both electrode active materials in capacitor.

in the concentrated electrolyte solutions (1–5 M). As the hydration number of Na^+ rises, the SC value for Na^+ adsorption on Maxsorb electrode decreases remarkably.

Fig. 8A shows the relationship between the freezing point and the salt concentration of the electrolyte solution. With the increase in salt concentration, the freezing point of electrolyte solution generally becomes lower. This fact hints that concentrated electrolyte solutions may be useful for "anti-frozen" electrochemical capacitors in cold environments. Fig. 8B compares the SC values of a Maxsorb electrode at the temperatures of 25 and −10 °C in the aqueous electrolyte solutions with various $NaClO_4$ concentrations. For each electrolyte solution, the SC value gets smaller as

the temperature drops down from 25 to −10 °C. Here we defined a parameter of R to estimate the retention extent of SC value as the temperature is lowered, which equals to the ratio of SC values at −10 to 25 °C. As the salt concentration rises, the R value becomes bigger. In addition, Fig. 8C shows galvanostatic charge and discharge curves of concentrated $NaClO_4$ (5 M) aqueous electrolyte solution at different temperatures. The discharge capacity retention can still reach to 80% even at −30 °C, compared with that at room temperature. This means that at certain low temperature, Maxsorb electrode can still deliver capacitance comparable to that at room temperature in the concentrated aqueous electrolyte solutions.

4. Conclusions

So far, we have shown many advantages of concentrated $NaClO_4$ aqueous solutions as the electrolytes for electrochemical capacitors. These virtues include:

1. High ionic conductivity of the electrolyte solutions results in a high rate capability (power density) of porous carbon electrode.
2. Decreased hydration number of ions in the electrolyte solutions leads to high specific capacitance (energy density) of porous carbon electrode.
3. Lowering the freezing point of an electrolyte solution is beneficial for the capacitive performance of porous carbon electrode at low temperatures.

Acknowledgements

This project was supported by the Foundation of Applied science and technology of Jilin Province (20090521), and Hundred Talents Program of Chinese Academy of Sciences.

References

[1] (a) H. Wang, M. Yoshio, A. Thapa, K.H. Nakamura, J. Power Sources 169 (2007) 375;
(b) H. Wang, M. Yoshio, Chem. Commun. 46 (2010) 1544.
[2] (a) L. Tian, A.B. Yuan, J. Power Sources 192 (2009) 693;
(b) L. Eliad, E. Pollak, N. Levy, G. Salitra, A. Soffer, D. Aurbach, Appl. Phys. A 82 (2006) 607.
[3] G.J. Wang, L.J. Fu, N.H. Zhao, Angew. Chem. Int. Ed. 46 (2007) 295.
[4] N.N. Sinha, P. Ragupathy, H.N. Vasan, N. Munichandraiah, Int. J. Electrochem. Sci. 3 (2008) 691.
[5] L.M. Chen, Q.Y. Lai, Y.J. Hao, Y. Zhao, X.Y. Ji, J. Alloys Compd. 467 (2009) 465.
[6] V. Khomenko, E. Raymundo-Pinero, F. Beguin, J. Power Sources 153 (2006) 183.
[7] V. Khomenko, E. Raymundo-Pinero, F. Beguin, Appl. Phys. A 82 (2006) 567.
[8] V. Ruiz, R. Santamaría, M. Granda, C. Blanco, Electrochim. Acta 54 (2009) 4481.
[9] N.R. Reddy, R.G. Reddy, J. Power Sources 124 (2003) 330.
[10] Y.U. Jeong, A. Manthiram, J. Electrochem. Soc. 149 (2002) 14.
[11] M.S. Hong, S.H. Lee, S.W. Kim, Electrochem. Solid-State Lett. 5 (2002) 227.
[12] K.W. Nam, C.W. Lee, X.Q. Yang, B.W. Cho, W.S. Yoon, K.B. Kim, J. Power Sources 188 (2009) 323.
[13] H.Y. Lee, S.W. Kim, H.Y. Lee, Electrochem. Solid-State Lett. 4 (2002) 19.
[14] Q.T. Qu, B.L. Wang, C. Yang, Y. Shi, S. Tian, Y.P. Wu, Electrochem. Commun. 10 (2008) 1652.
[15] Y.G. Wang, Y.Y. Xia, Electrochem. Commun. 16 (2005) 1138.
[16] Q.T. Qu, P. Zhang, B. Wang, Y.H. Chen, S. Tian, Y.P. Wu, R. Holze, J. Phys. Chem. C 113 (2009) 14020.
[17] A. Malak, K. Fic, G. Lota, C. Vix-Guterl, E. Frackowiak, J. Solid-State Electrochem. 14 (2010) 811.
[18] N.L. Wu, S.Y. Wang, J. Power Sources 110 (2002) 233.
[19] K.R. Prasad, N. Miura, Electrochem. Commun. 6 (2004) 849.
[20] K.R. Prasad, N. Miura, Electrochem. Commun. 6 (2004) 1004.
[21] K.R. Prasad, N. Miura, Electrochem. Solid-State Lett. 425 (2004) 428.
[22] M. Toupin, T. Brousse, D. Belanger, Chem. Mater. 14 (2002) 3946.
[23] J.Y. Luo, Y.Y. Xia, J. Electrochem. Soc. 154 (2007) 987.
[24] K.R. Prasad, N. Miura, J. Power Sources 135 (2004) 354.
[25] X.H. Yang, Y.G. Wang, H.M. Xiong, Y.Y. Xia, Electrochim. Acta 53 (2007) 752.
[26] T. Brousse, M. Toupin, D. Belanger, J. Electrochem. Soc. 151 (2004) 614.
[27] T. Brousse, P.L. Taberna, O. Crosnier, R. Dugasa, P. Guillemet, Y. Scudeller, Y. Zhou, F. Favier, D. Belanger, P. Simon, J. Power Sources 173 (2007) 633.
[28] T. Cottineau, M. Toupin, T. Delahaye, T. Brousse, D. Belanger, Appl. Phys. A 82 (2006) 599.
[29] J.P. Zheng, T.R. Jow, J. Electrochem. Soc. 144 (1997) 2417.
[30] J.P. Zheng, J. Huang, T.R. Jow, J. Electrochem. Soc. 144 (1997) 2026.
[31] J.P. Zheng, J. Electrochem. Soc. 150 (2003) 484.
[32] L.R. Faulkner, Electrochemical Methods: Fundamentals and Applications, 2nd ed., John Wiley & Sons, Inc., 2001, p. 13.
[33] J.S. Huang, B.G. Sumpter, V. Meunier, Angew. Chem. Int. Ed. 47 (2008) 520.
[34] C. Zheng, L. Qi, M. Yoshio, H. Wang, J. Power Sources 195 (2010) 4406.
[35] Y. Chen, Y.H. Zhang, L. Zhao, J. Phys. Chem. Chem. Phys. 6 (2004) 537.
[36] Y.H. Zhang, C.K. Chan, J. Phys. Chem. A 107 (2003) 5956.
[37] X.P. Xuan, J.J. Wang, J.S. Lu, N. Pei, Y. Mo, J. Spectrochim. Acta. A 57 (2001) 1555.
[38] D.W. James, R. Ayes, Aust. J. Chem. 35 (1998) 1775.
[39] D.W. James, R.E. Mayes, Aust. J. Chem. 35 (1998) 1785.
[40] R.H. Li, Z.P. Jiang, Y.T. Guan, H.W. Yang, B. Liu, J. Raman Spectrosc. 40 (2009) 1200.
[41] M. Morita, Y. Asai, N. Yoshimoto, M. Ishikawa, J. Chem. Soc. Faraday Trans. 94 (1998) 34.
[42] Y. Yamada, Y. Takazawa, K. Miyazaki, T. Abe, J. Phys. Chem. C 114 (2010) 11680.